Finite difference time domain analysis of two-dimensional surface acoustic wave piezoelectric phononic crystals at radio frequency*

TIAN Yahui[1] LI Honglang[1] KE Yabing[1] LUO Wei[3] WEI Jiangbo[2] HE Shitang[1]

(1 *Institute of Acoustics, Chinese Academy of Sciences* Beijing 100190)

(2 *Information-Electric Institute, MESNAC co., ltd.* Qingdao 266045)

(3 *School of Optical and Electrical Information, Huazhong Univ. of Science & Technology* Wuhan 430074)

Received Sept. 17, 2014

Revised Nov. 4, 2014

Abstract The finite-difference time-domain (FDTD) method is proposed for analyzing the surface acoustic wave (SAW) propagation in two-dimensional (2D) piezoelectric phononic crystals (PCs) at radio frequency (RF), and also experiments are established to demonstrate its analysis result of the PCs' band gaps. The FDTD method takes the piezoelectric effect of PCs into account, in which periodic boundary conditions are used to decrease memory/time consumption and the perfectly matched layer boundary conditions are adopted as the SAW absorbers to attenuate artificial reflections. Two SAW delay lines are established with/without piezoelectric PCs located between interdigital transducers. By removing several echoes with window gating function in time domain, delay lines transmission function is achieved. The PCs' transmission functions and band gaps are obtained by comparing them in these two delay lines. When Aluminum/128°YX-$LiNbO_3$ is adopted as scatter and substrate material, the PCs' band gap is calculated by this FDTD method and COMSOL respectively. Results show that computational results of FDTD agree well with experimental results and are better than that of COMSOL.

PACS numbers: 43.35, 43.60

DOI: 10. 15949/j. cnki. 0217-9776. 2015. 03. 006

1 Introduction

Similar to light in photonic crystals, phononic crystals (PCs)[1] are periodic elastic structures with arrays of scattering inclusions located in a homogeneous host material, which has

* This work was supported by the National Natural Science Foundation of China (11174318, 11304346, 61106081), Chinese Postdoctoral Science Foundation (2011M501204, 2013T60718), National High Technology Research and Development Program (863 Program) (SS2013AA041103), Beijing Municipal Science and Technology Commission Project (Z141100003814016), the Fundamental Research Funds for the Central Universities (HUST: 2013QN038).

band gaps with acoustic waves completely reflected in these certain frequencies. As the acoustic waves in PCs have a low velocity of ten millionth of the speed of light, PCs are fabricated in micro-nanometer size and widely used in radio frequency (RF, MHz-GHz) devices, such as surface acoustic wave (SAW) filter and bulk acoustic wave (BAW) filter, which are called one-dimensional PCs. Recently, two-dimensional (2D) piezoelectric PCs have more attractive features such as multi-forbidden bands[2], high reflection and localized state control [3−4], ultra broadband[5], negative refraction[6], low loss[7] and acoustic focus[8], which show good prospect in application of 2D acoustic functional devices[8−11].

Plane wave expansion[12−16] (PWE), finite element method[17−22] (FEM), finite-difference-time domain[23−26] (FDTD) are used for analysis of SAW propagation in 2D piezoelectric PCs. PWE was used by Vincent Laude[12] to calculate the complete band gaps of SAW in air/128° YX-$LiNbO_3$ PCs[16], which is simple but is with little decreaced accuracy due to its slow convergence. FEM was used by S.Benchaba [17] and Rupp.C.J[18] to analyze the same structure, which is high accuracy but has large consuming time and memory.

Compared with PWE and FEM, FDTD method have been demonstrated to be both simple and efficiency for analyzing PCs in Hz and kHz frequency range by Jia-Hong Sun[23] and Li Jinqiang[24], who had successfully used FDTD to analyze the band gaps in steel/epoxy PCs and barium titanate/polymer PCs. However, FDTD analysis of PCs in MHz-GHz frequency range is still in the exploratory stage.

In this paper, the FDTD theoretical model of considering piezoelectric effect of PCs was firstly presented to analyze SAW propagation in the 2D piezoelectric PCs at RF range. The periodic boundary conditions and the perfect matching layer (PML) absorbing boundary conditions were adopted by the FDTD model. Then experiments were established to verify the FDTD theory. Through measuring the responses of two structures of delay line (one with PCs in the transmission path, another without), the transmission coefficients of SAW in the 2D piezoelectric PCs was obtained. Furthermore, to verify the efficiency and accuracy of the FDTD, the FEM model with commercial software COMSOL was also used to calculate the band gaps of 2D piezoelectric PCs.

2 FDTD model of 2D piezoelectric PCs

Figure 1 illustrates the FDTD model of 2D piezoelectric PCs to analyze band gaps in the x direction. In the model, piezoelectric effect was taken into account in the FDTD differential equations. To reduce the memory and time cost, periodic boundary condition was used to simulate infinite periodic structure of piezoelectric PCs in the y direction. While in the x direction, the PCs are finite, and excitation signal source and signal receiver are placed on the two sides respectively. To attenuate the artificial reflection of both sides in the x direction, PML boundary conditions were used to achieve the complete absorption of SAW. By comparing the excited and received signal spectral, the transmission coefficients of the piezoelectric PCs in the x direction was achieved, and then the band gaps were obtained. Using the same method, the transmission coefficients of the piezoelectric PCs in the y direction was also obtained.

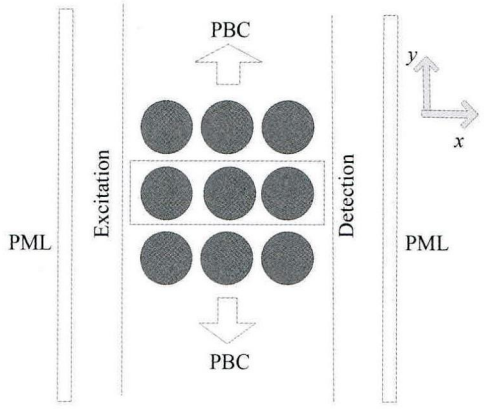

Fig. 1 The FDTD model of the 2D piezoelectric PCs.

2.1 FDTD differential equations for piezoelectric PCs

The SAW propagating in piezoelectric PCs satisfies piezoelectric constitutive equations and Newton's motion equation[27]. From these equations, FDTD differential equations are deduced as formula (1), here assuming that SAW is located in the x-y plane and propagates along the x direction.

$$\begin{cases} \rho\dfrac{\partial v_1}{\partial t} = \dfrac{\partial T_{11}}{\partial x_1} + \dfrac{\partial T_{13}}{\partial x_3}, \\ \rho\dfrac{\partial v_3}{\partial t} = \dfrac{\partial T_{33}}{\partial x_1} + \dfrac{\partial T_{13}}{\partial x_3}, \\ \dfrac{\partial T_{11}}{\partial t} = c_{33}^D\dfrac{\partial v_1}{\partial x_1} + c_{13}^D\dfrac{\partial v_3}{\partial x_3}, \\ \dfrac{\partial T_{33}}{\partial t} = c_{13}^D\dfrac{\partial v_1}{\partial x_1} + c_{11}^D\dfrac{\partial v_3}{\partial x_3}, \\ \dfrac{\partial T_{13}}{\partial t} = c_{44}^D\dfrac{\partial v_1}{\partial x_3} + c_{44}^D\dfrac{\partial v_3}{\partial x_1}, \end{cases} \tag{1}$$

where $\boldsymbol{T}$ is the stress; $\boldsymbol{V}$ is the velocity; c is the elastic tensor; ε^s is the dielectric constant; e is the piezoelectric constant and ρ is the density. For isotropic media, piezoelectric constant e is 0. Here, $c_{33}^D = c_{33}^E + e_{33}^2/\varepsilon_{33}$, $c_{13}^D = c_{13}^E + e_{33}e_{13}/\varepsilon_{33}$, $c_{11}^D = c_{11}^E + e_{31}^2/\varepsilon_{33}$, $c_{44}^D = c_{44}^E + e_{15}^2/\varepsilon_{11}$, these equivalent elastic constants takes the piezoelectric effect into account.

2.2 PML absorbing boundary condition

The virtual reflection at either side of the PCs can destroy the simulation results. In order to attenuate this reflection, PML absorbing boundary conditions are adopted. PML is composed by a high lossy media in which the wave transmitting decays quickly. With appropriate finite thickness of PML, the transmission waves can be well absorbed. In PML area, the decay of the wave is determined by the attenuation factor which is commonly used as formula (2)[28]:

$$\sigma(x) = \sigma_{\max}\left(\frac{x}{d}\right)^2, \tag{2}$$

where d is the thickness of the PML layer; x denotes the distance between the inner boundaries of PML area and $\sigma_{\max}$ is the maximum attenuation value in the outer boundary of the PML area.

FDTD differential equations in PML area have deduced from FDTD differential equation in PCs by introducing the attenuation factor of formula (2). In this paper, V_x of velocity vectors in the PML area was deduced as formula (3).

$$\begin{cases} V_x^x \Big|_{i,j+1/2}^{n+1/2} = \dfrac{2-\sigma_i^x \Delta t}{2+\sigma_i^x \Delta t} V_x^x \Big|_{i,j+1/2}^{n+1/2} + \dfrac{2\Delta t}{2+\sigma_i^x \Delta t} \dfrac{T_{xx}\Big|_{i+1/2,j+1/2}^{n} - T_{xx}\Big|_{i-1/2,j+1/2}^{n}}{\rho \Delta x}, \\ V_x^y \Big|_{i,j+1/2}^{n+1/2} = \dfrac{2-\sigma_{j+1/2}^y \Delta t}{2+\sigma_{j+1/2}^y \Delta t} V_x^x \Big|_{i,j+1/2}^{n+1/2} + \dfrac{2\Delta t}{2+\sigma_{j+1/2}^y \Delta t} \dfrac{T_{xx}\Big|_{i,j+1}^{n} - T_{xx}\Big|_{i,j}^{n}}{\rho \Delta x}, \\ V_x \Big|_{i,j+1/2}^{n+1/2} = V_x^x \Big|_{i,j+1/2}^{n+1/2} + V_x^y \Big|_{i,j+1/2}^{n+1/2}, \end{cases} \tag{3}$$

where i, j represents the coordinate in the x and y direction respectively, n represents the time coordinate and ρ is the mass density. Similarly, FDTD differential equations of V_y and three stress components in PML area can also be obtained.

2.3 Periodic boundary conditions

In the y direction, the periodic boundary conditions were utilized to restrict the sound waves on both sides, which are illustrated as formula (4)[29]:

$$\begin{cases} V_x\left(0, j-\dfrac{1}{2}\right) = V_x\left(0, a_1+j-\dfrac{1}{2}\right), \\ V_y\left(\dfrac{1}{2}, j\right) = V_y\left(\dfrac{1}{2}, a_1+j\right), \\ T_{xx}\left(\dfrac{1}{2}, j-\dfrac{1}{2}\right) = T_{xx}\left(\dfrac{1}{2}, a_1+j-\dfrac{1}{2}\right), \\ T_{yy}\left(\dfrac{1}{2}, j-\dfrac{1}{2}\right) = T_{yy}\left(\dfrac{1}{2}, a_1+j-\dfrac{1}{2}\right), \\ T_{xy}(0, j) = T_{xy}(0, a_1+j), \end{cases} \tag{4}$$

where a_1 and j represents the lattice constant and the coordinate in the y direction respectively.

3 Experimental verification of FDTD analysis

In order to confirm the validity of FDTD method, experiments were designed with two delay line structures as shown in Fig. 2. Figure 2(a) is one delay line structure without PCs. Figure 2(b) is another delay line structure with PCs constructed by aluminum/128° YX-$LiNbO_3$. By measuring the responses of these two structures, transmission coefficients of 2D piezoelectric PCs can be obtained.

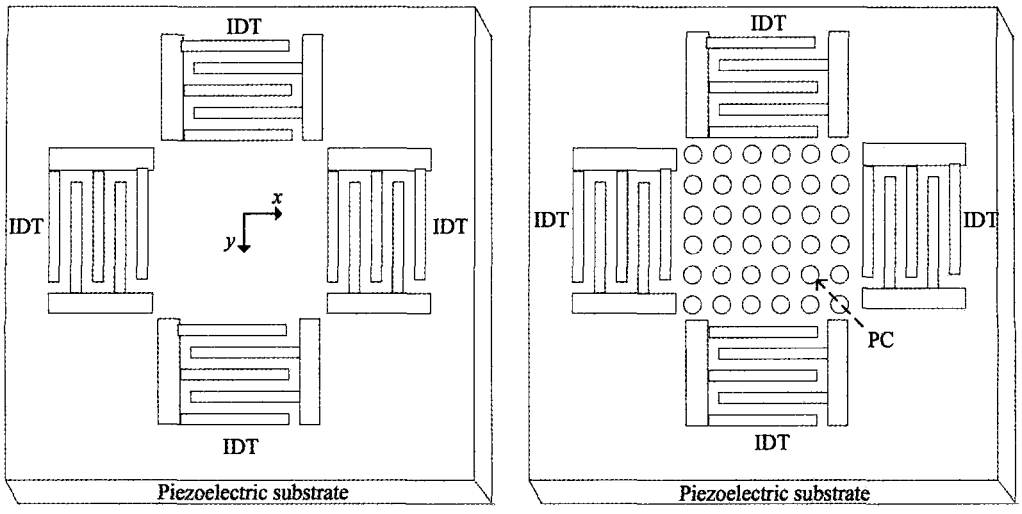

(a) Delay line structure without PCs (b) Delay line structure with PCs

Fig. 2 The structures of the experiments.

3.1 Parameters in experiments

In experiments, 128° YX-$LiNbO_3$ was used as piezoelectric substrate. Through calculating the effective permittivity of the substrate, the electromechanical coupling coefficients is 5.4% in the x direction and 1.1% in the y direction, indicating that SAW can be efficiently excited in both directions.

In the structure of 2D piezoelectric PCs constructed by aluminum/128° YX-$LiNbO_3$, the lattice period is 10 μm and the diameter of aluminum cylinders is 7 μm. The period of the interdigital transducers (IDT) is 12 μm and metallization ratio is 0.5. The thickness of the IDT film and aluminum cylinders is 6000 Angstroms. In experiments, responses of the delay line structures (with/without PCs) were measured by network analyzer. To remove several echoes (multiple reflection signals etc.), window gating function in time domain was used to retain the first transmitting signal. Subtracting transmission coefficients of these two structures, the band gaps of the piezoelectric PCs were derived.

3.2 Comparison of experimental and theoretical results

Figure 3 illustrates the transmission coefficients measured by experiments in the x direction. It can be clearly found that the transmission coefficient of the structure with PCs is significantly small in the vicinity of 197 MHz and 300 MHz, which are band gaps of piezoelectric PCs.

To further verify the accuracy of FDTD method, finite element software COMSOL was used to calculate the transmission coefficients of the PCs. Figure 4 illustrates the transmission coefficients of the piezoelectric PCs in the x direction by COMSOL and FDTD method respectively. A larger deviation appeared in the low frequency range, which may result from the rough mesh in COMSOL limited by the computing time and memory capacity[30]. The band gap calculated by COMSOL in this range will be ignored.

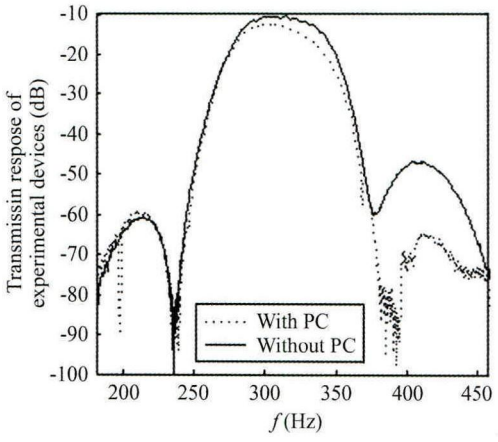

Fig. 3 Frequency responses of delay line structures in experiments of the x direction.

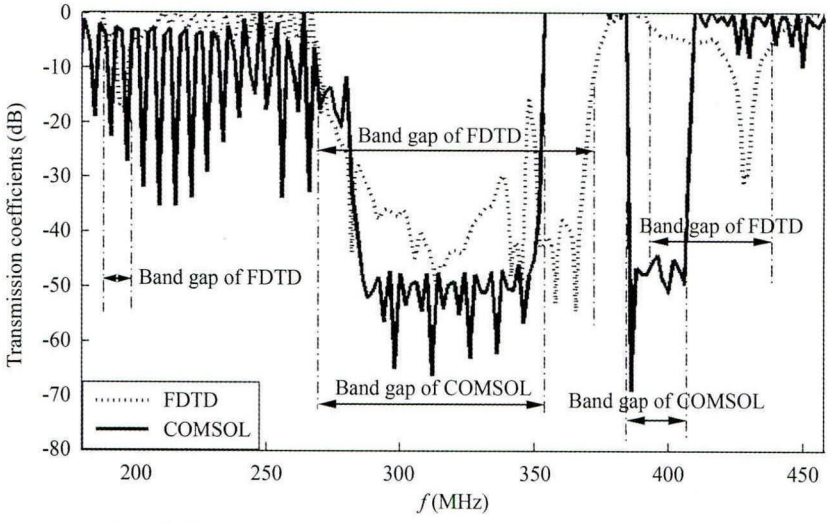

Fig. 4 Transmission coefficients calculated by FDTD and COMSOL.

Figure 5 denotes the transmission coefficients of the piezoelectric PCs in the x direction obtained by experiments and FDTD calculation respectively. Table 1 shows the derived band gaps of the experiments and the FDTD calculation from Fig. 5. Three close band gaps obtained by FDTD are similar to the experiment, which indicates the FDTD calculation is efficient. However, the deviations in the first band gap and the third band gap exist, and the second band gap of experiments is not obvious compared with calculation, which are caused by that the mass-loading effect of the metal cylinders is not be considered in the two-dimensional FDTD calculation model

Similarly Fig. 6 illustrates the transmission coefficients of the two experimental delay line structures in the y direction. Figure 7 displays the transmission coefficients of piezoelectric PCs in the y direction calculated by FDTD and COMSOL method respectively. Figure 8 shows the transmission coefficients of piezoelectric PCs in the y direction obtained by experiments and FDTD calculation respectively. Table 1 lists the band gaps obtained from Fig. 8. Four band gaps are obtained by FDTD calculation in which the last three ones is close to the experimental results, while the first band gap was not found in experiments, which is because of large noise

in experiments and the ignoring of the thickness of the metal cylinders.

Table 1 lists the band gaps obtained by experiments, FDTD calculation and COMSOL calculation respectively. Firstly the band gaps in the x direction is analyzed. The first band

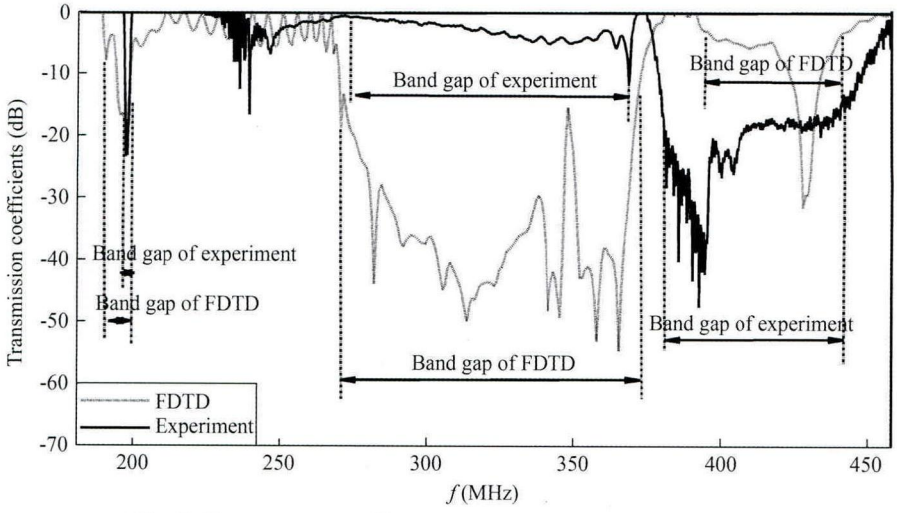

Fig. 5 Transmission coefficients in the x direction of piezoelectric PCs.

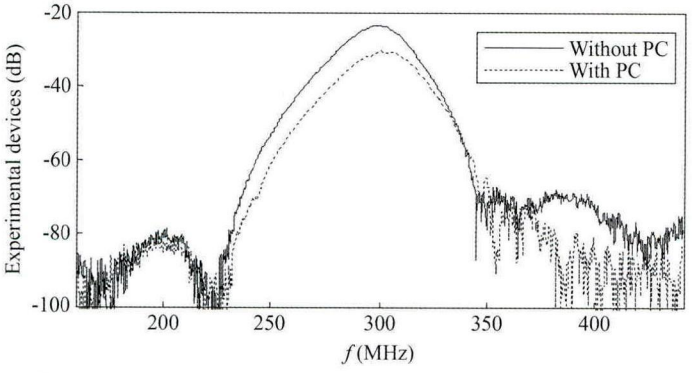

Fig. 6 Frequency response of delay line structures in the y direction of experiments.

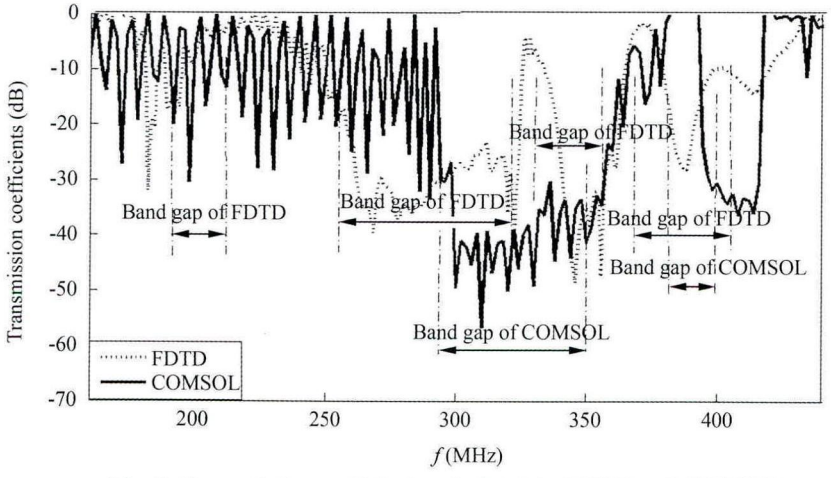

Fig. 7 Transmission coefficients calculated by FDTD and COMSOL.

gap is obtained by FDTD while not by COMSOL . The second band gap obtained by FDTD is more close to experiments than that of COMSOL. The third band gap calculated by COMSOL is in low frequency range while it's in high frequency range by FDTD calculation, compared to experiments. Secondly the band gaps in the y direction is analyzed. The first band gap is still not obtained by COMSOL calculation. The second band gap, the third band gap and the fourth band gap calculated by FDTD are also more close to experiments than that of COMSOL calculation. As a consequence, the precision of FDTD calculation is superior to COMSOL calculation.

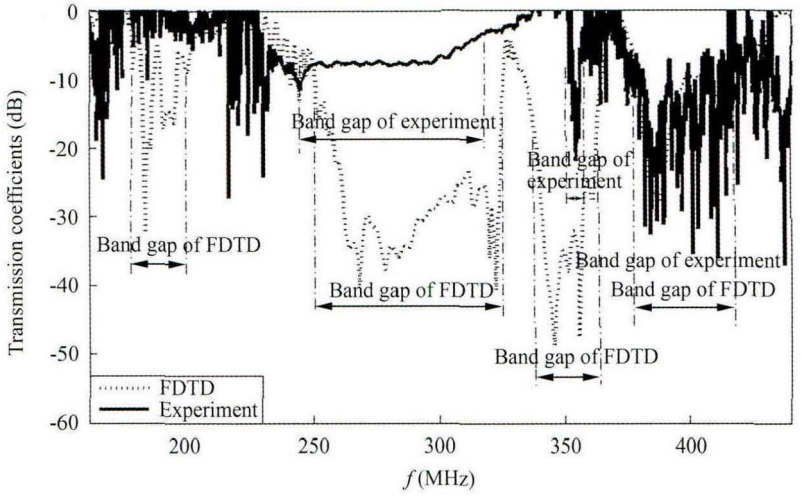

Fig. 8 Transmission coefficients in the y direction of piezoelectric PCs.

Table 1 The comparison of band gaps from experiments, FDTD calculation and COMSOL calculation

		First band gap	Second band gap	Third band gap	Fourth band gap
x direction	Experiments	196~199 MHz	275~370 MHz	380~440 MHz	
	FDTD	190~200 MHz	270~375 MHz	400~440 MHz	
	COMSOL		270~355 MHz	385~410 MHz	
y direction	Experiments		240~310 MHz	352~360 MHz	380~420 MHz
	FDTD	175~200 MHz	250~320 MHz	335~365 MHz	380~420 MHz
	COMSOL		295~360 MHz		390~415 MHz

The deviations between experiments and FDTD calculation are mainly due to two reasons: Firstly, the model used by FDTD calculation was assumed that the thickness of the aluminum cylinders was infinite, while the actual thickness in experiments was limited with less than one wavelength. Secondly, the spectrum bandwidth of the delay line in experiments is too small to cover the whole analyzing spectrum, resulting in the inaccurate measurements outside the passband. These reasons will be further studied in the future works.

4 Conclusions

In this paper, band gaps of SAW in the 2D piezoelectric PCs in RF range was studied. In theory, FDTD method was established by introducing PML and periodic boundary conditions.

In experiments, the transmission cofficients of PCs were obtained by the method of subtraction of two delay line structures (with/without PCs) and window gating function in time domain. In addition, by comparing the results of FDTD, COMSOL and experiments, it showd that FDTD is the more advantageous method for 2D piezoelectric PCs. Due to 2D FDTD model didn't consider the finite thickness of cylinders, three-dimensional FDTD model is needed.

References

[1] Wu Fugen, Liu Zhengyou, Liu Youyan. The band gaps in two-dimensional composite media. *Acta Acustica* (In Chinese), 2001; **26**(4): 319–323

[2] Mohammadi S, Eftekhar A A, Khelif A, Hunt W D. Evidence of large high frequency complete phononic band gaps in silicon phononic crystal plates. *Applied Physics Letters*, 2008; **92**(22): 221905

[3] Wang Lin, Tao Zhiyong, Wang Xinlong. Defect states in the non-Bragg band gap. *Acta Acustica* (In Chinese), 2011; **36**(2): 202–206

[4] Olsson R H, El-Kady I. Microfabricated phononic crystal devices and applications. *Measurement Science and Technology*, 2009; **20**(1): 012002

[5] Soliman Y M, Su M F, Leseman Z C, Reinke C M, El-Kady I, Olsson R H. Phononic crystals operating in the gigahertz range with extremely wide band gaps. *Applied Physics Letters*, 2010; **97**(19): 193502

[6] Zhang X, Liu Z. Negative refraction of acoustic waves in two-dimensional phononic crystals. *Applied Physics Letters*, 2004; **85**(2): 341–343

[7] Solal M, Gratier J, Kook T. A SAW resonator with two-dimensional reflectors. Frequency Control Symposium, 2009 Joint with the 22nd European Frequency and Time forum. IEEE International, 2009: 226–231

[8] Wu Tsungtsong, Tang Hetai, Chen Yungyu, Liu Peiling. Analysis and design of focused interdigital transducers. *Ultrasonics, Ferroelectrics and Frequency Control, IEEE Transactions on*, 2005; **52**(8): 1384–1392

[9] Wu Tsungtsong, Wang Weishan, Sun Jiahong. A layered SAW device using phononic-crystal reflective gratings. IEEE International Ultrasonics Symposium Proceedings, 2008: 709–711

[10] Benchabane S, Khelif A, Daniau W, Robert L, Pétrini V, Assouar B, Vincent B, Elmazria O, Krüger J, Laude V. Silicon phononic crystal for surface acoustic waves. IEEE Ultrasonics Symposium, 2005: 922–925

[11] Mohammadi S, Eftekhar A A, Hunt W D, Adibi A. Demonstration of large complete phononic band gaps and waveguiding in high-frequency silicon phononic crystal slabs. IEEE International Ultrasonics Symposium Proceedings, 2008: 768–772

[12] Laude V, Wilm M, Benchabane S, Khelif A. Full band gaps for surface acoustic waves in piezoelectric phononic crystals. IEEE Ultrasonics Symposium, 2004: 1046–1049

[13] Huang Ziggui, Wu Tsungtsong. Analysis of surface acoustic wave propagation in phononic crystal waveguides using FDTD method. IEEE Ultrasonics Symposium, 2005: 77–80

[14] Hsu Jin Chen, Wu Tsung Tsong. A fast algorithm for calculating band structures in two-dimensional phononic-crystal plates. IEEE Ultrasonics Symposium, 2006: 1169–1176

[15] Wu Tsungtsong, Wu Liangchen, Huang Zigui. Frequency band-gap measurement of two-dimensional air/silicon phononic crystals using layered slanted finger interdigital transducers. *Journal of Applied Physics*, 2005: 094916–094916-7

[16] Wu Tsungtsong, Hsu Zinchen, Huang Zigui. Band gaps and the electromechanical coupling coefficient of a surface acoustic wave in a two-dimensional piezoelectric phononic crystal. *Physical Review B*, 2005; **71**(6): 064303

[17] Benchabane S, Khelif A, Rauch J Y, Robert L, Laude V. Evidence for complete surface wave band gap in a piezoelectric phononic crystal. *Phys Rev E Stat Nonlin Soft Matter Phys*, 2006; **73**(6): 065601

[18] Rupp C J, Evgrafov A, Maute K, Dunn M L. Design of phononic materials/structures for surface wave devices using topology optimization. *Structural and Multidisciplinary Optimization*, 2007; **34**(2): 111–121

[19] Hladky Hennion A C, Vasseur J, Dubus B. Analysis of signals propagating in a phononic crystal PZT layer deposited on a silicon substrate. *IEEE Transactions on Ultrasonics, Ferroelectrics, and Frequency Control*, 2013: 2607–2616

[20] Sun Jiahong, Wu Tsungtsong. High efficiency phononic crystal reflective gratings for surface acoustics waves. IEEE International Ultrasonics Symposium Proceedings, 2011: 996–999

[21] Badreddine Assouar M, Mourad Oudich. Dispersion curves of surface acoustic waves in a two-dimensional phononic crystal. *Applied Physics Letters*, 2011: 123505–123505-3

[22] Pashchenko V P. Surface acoustic wave ferroelectric phononic crystal tunable by electric field. *Nanosystems: Physics, Chemistry, Mathematics*, 2013; **4**(5): 630–634

[23] Sun Jiahong, Wu Tsungtsong. Propagation of surface acoustic waves through sharply bent two-dimensional phononic crystal waveguides using a finite-difference time-domain method. *Physical Review B*, 2006; **74**(17): 174305

[24] Li Jinqiang, Li Fengming, Wang Yuesheng, Kishimoto K. Wave propagation in two-dimensional disordered piezoelectric phononic crystals. *Acta Mechanica Solida Sinica*, 2008; **21**(6): 507–516

[25] Wu Tsungtsong, Wang Weishan, Sun Jiahong. A layered SAW device using phononic-crystal reflective gratings. IEEE Ultrasonics Symposium Proceddings, 2008: 709–712

[26] Wu Tsungtsong, Sun Jiahong. Band gap materials and micro-phononic devices. Frequency Control Symposium, 2010: 515–520

[27] Wong Kingyuen. Analysis of SAW filters using finite-difference time-domain method. Hong Kong: Polytechnic University, 2005: 23–90

[28] Allen T. Computational electrodynamics: the finite difference time domain method. Second Edition. Boston London: Artech House, 2000: 285–625

[29] Wen Xisen, Wen Jihong, Yu Dianlong, Wang Gang, Liu Yaozong, Han Xiaoyun. Phononic crystals. Beijing: National Defense Industry Press, 2009: 29–35

[30] louvet carron T, Leost J. FEMthermal analysis of quartz oscillator with COMSOL. IEEE International Frequency Control Symposium, 2009 Joint with the 22nd European Frequency and Time forrum, 2009: 482–486